



2019 16th International Conference on
Quality in Research (QIR):
International Symposium on
Electrical and Computer Engineering
Padang Convention Center, 22–24 July 2019

2019 16th International Conference on Quality in Research (QIR): International Symposium on Electrical and Computer Engineering

22 - 24 July 2019

Padang, Indonesia

Organized by:



Faculty of

Engineering

Co-hosted by:



XPLORE COMPLIANT

IEEE Catalog Number : CFP19QIR-ART

ISBN : 978-1-7281-1898-7



**2019 16th International Conference on
Quality in Research (QIR):
International Symposium on
Electrical and Computer Engineering**
Padang Convention Center, 22–24 July 2019

CONFERENCE ORGANIZER

ADVISOR

- Dr. Ir. Hendri D.S. Budiono, M.Eng. , Universitas Indonesia
- Ir. Insannul Kamil, M.Eng, Ph.D , Universitas Andalas

GENERAL CHAIR

Dr. Eng. Muhamad Sahlan , Universitas Indonesia

CO-CHAIR

Dr. Yudan Wulanza , Universitas Indonesia

INTERNATIONAL ADVISORY BOARD

- Prof. Benny Tjahjono , Coventry University
- Prof. Suk Young Kim , Yeungnam University South Korea
- Assoc. Prof. M. Akbar Rhamdani , Swinburn University Australia
- Prof. Ray-Guang Cheng , National Taiwan University of Science
- Prof. Shi-Woei Lin , National Taiwan University of Science
- Dr. Aya Hagishima, Kyushu University
- Prof. Afshin J. Ghajar, Ph.D., P.E., (School of Mechanical and Aerospace Engineering, Oklahoma State University)
- Prof. Diego Ramirez-Lovering, Monash University
- Associate Professor. David McCarthy, Monash University, Australia
- Prof. Samuel Kinde Kassegne, Ph.D, PE, San Diego State University
- Dr. Jerome Charmet, University of Warwick

STEERING COMMITTEE

- Dr. Ir. Muhamad Asvial, M.En.g , Universitas Indonesia
- Prof. Dr.Ing. Nandy Putra , Universitas Indonesia
- Dr. Dwi Marta Nurjaya, S.T, M.T. , Universitas Indonesia
- Jos Istiyanto, S.T., M.T., Ph.D. , Universitas Indonesia
- Dr. Eng. Arief Udhiarto, S.T., M.T., IPM. , Universitas Indonesia
- Dr. Ir. Imansyah Ibnu Hakim, M.Eng. , Universitas Indonesia
- Dr. Badrul Munir, ST., M.Eng.Sc. I Universitas Indonesia
- Prof. Dr. Ir. Riri Fitri Sari, M.M. M.Sc. , Universitas Indonesia
- Prof. Dr. Anne Zulfia, M.Sc. , Universitas Indonesia
- Dr. Ir. Nahry, M.T. , Universitas Indonesia
- Dr. Ir. Yuliusman , Universitas Indonesia
- Ir. Evawani Ellisa, M.Eng. Ph.D , Universitas Indonesia
- Ardiansyah, Ph.D. , Universitas Indonesia
- Prof. Dr. Eng. Gunawarman , Universitas Andalas
- Ir. Taufik, MT. , Universitas Andalas
- Dr. Is Prima Nanda, MT. , Universitas Andalas
- Dr. Hendra Suherman , Universitas Bung Hatta



**2019 16th International Conference on
Quality in Research (QIR):
International Symposium on
Electrical and Computer Engineering**
Padang Convention Center, 22–24 July 2019

CONFERENCE ORGANIZER

SCIENTIFIC PUBLICATION PARTNER

- Dr. Eng. Radon Dhelika, B.M. Eng. , Universitas Indonesia
- Eny Kusrini, Ph.D. , Universitas Indonesia
- Dr. Eng. Reni Desmiarti , Universitas Bung Hatta

TECHNICAL PROGRAM COMMITTEE

- Wahyuaji N. Putra, ST., M.T. , Universitas Indonesia
- Ajib Setyo Arifin, ST., MT., Ph.D , Universitas Indonesia
- Dr. Ing. Yulia N. Harahap, ST. M.Des.S. , Universitas Indonesia
- Dr. Oknovia Susanti , Universitas Andalas
- Elita Amrina, Ph.D. , Universitas Andalas
- Dr. Aulia , Universitas Andalas
- Dr. Eng. Zulkarnaini , Universitas Andalas
- Nurhamidah, M.Eng. , Universitas Andalas
- Dr. Jonny Wongso , Universitas Bung Hatta
- Islahuddin, M.T. , Universitas Dharma Andalas
- Ridho Aidil Fitrah, M.T. , Universitas Dharma Andalas

SPONSORSHIP COMMITTEE

- Annisa Marlin, ST., MSc. , Universitas Indonesia

Conference Organizing Committee :

Organizing Committee Secretariat
Dean's Building, 2nd Floor
Faculty of Engineering,
Universitas Indonesia 16424
Depok, West Java Indonesia
Phone : +62-21-7863504
e-mail : qir@eng.ui.ac.id





Table of Content

Integration of localized surface plasmon resonance and electrochemical sensors for liquid environmental monitoring	1
Implementation of Ziegler-Nichols PID Tuning Method on Stabilizing Temperature of Hot-water Dispenser	5
Three Mixture of Odor Classification using Convolutional Neural Network	10
The Back-propagation Neural Network Classification of EEG Signal Using Time Frequency Domain Feature Extraction	14
Semi Active Control of Solar Tracker Using Variable Position of Added Mass Control	18
Implementation of Artificial Neural Network: Back Propagation Method on Face Recognition System	23
Analysis of the IEEE 802.15.4 Protocol with Rabbit Encryption Algorithm for Industrial Applications in Oil and Gas Sector	28
Conserving RACH Energy Usage with Flexible Preamble Allocation for IoT Coexisting with H2H Services	33
Visualization of Time Series Data Change by Statistical Shape Analysis	39
NB-IoT Network Planning for Smart Metering services in Jakarta, Depok, Tangerang and Bekasi	45
Validation of 3D Models using Template Matching for Implant Planning	51
Multiparty Zero-Knowledge Protocol for User Authentication on Android	55
ATmega16 Microcontroller-based Automatic Coffee Brewing System using Pour Over V60 Technique	60
Real-Time Classification for Cardiac Arrhythmia ECG Beat	64
Upgrading Mobile Network to 5G: The Technoeconomic Analysis of Main Cities in Indonesia	69
Hyperspectral Unmixing Using L2,1 Norm and Total Variation for Material Detection on Earth's Surface	75
Energy Consideration for Wireless Sensor Network	79
Effects of Substrate Curvature in Performances of Conformal Microstrip Arrays	83
Correcting Block Attack on Reduced NEEVA	87
Compact UWB Bandpass Filter based on Crossed Dumbbell-Stub with Notch Band using Defected Microstrip Structure	92
Flashover Phenomenon on 150kV Transmission Line Due to Direct Lightning Strike on the Ground Wire	97
Analysis of Concrete Inspection Radar Equations to Obtain Radar System Specifications	102
A Compact Right Hand Circular Polarization Microstrip Antenna using Inverted-L Shaped Feedline for GPS Receiver	106
Answer Categorization Method with K-Means for Automatic Short Answer Grading System for Indonesian Language Based on Latent Semantic Analysis	110
Review Supercapacitor Using Active Carbon Electrode	115
Performance Analysis of Data Transmission on WebSocket for Real-time Communication	123
Collision Attack on 4 Secure PGV Hash Function Schemes based on 4-Round PRESENT-80 with Iterative Differential Approach	128
Study on Sustainability of Indonesia 2G Operator	132
Characteristics of Lead-Acid Battery Charging and Discharging Against Residential Load in Tropical Area	137
Gait Analysis for Biometric Surveillances Using Kinect™: A Study Case of Axial Skeleton Movements	143
A Tool for Making Segmented Speech Corpus for ASR and TTS Modeling	147



**2019 16th International Conference on
Quality in Research (QIR):
International Symposium on
Electrical and Computer Engineering**

Padang Convention Center, 22–24 July 2019

Data Acquisition for Rocket Control with Aircraft Simulator X-Plane and MATLAB	151
Performance Evaluation of Query Response Time in The Document Stored NoSQL Database	156
Security System Design on Feature Information of Biometric Fingerprint using Kronecker Product Operation and Elementary Row Operation	162
Simulation and Analysis of a Buck Converter Based on an Arduino PWM Signal Using a Single Cell Li-Ion Load	167
Smart City Reseach in Indonesia: A Bibliometric Analysis	172
K-Means Clustering for Answer Categorization on Latent Semantic Analysis Automatic Japanese Short Essay Grading System	177
Surface Current Analysis of THz Bowtie Antenna-coupled Microbolometer	182
Improving Wireless Power Transfer Performance by Partitioned Shielding	186
A Novel Design Retangular UWB Antena Array for Microwave Breast Tumor Detection	190
New Design of 60-GHz Quasi-Yagi and Stacked Series Planar Antenna Array for 5G Wireless Application	195
Impact of Downscaling on Terahertz Antenna-Coupled Bolometers	201
Room-Temperature Terahertz Antenna-Coupled Microbolometers with Titanium Thermistor and Heater	205
Enhancement Bandwidth of Parasitic Microstrip Antenna Using Multiple Feed Line	210
Optimization Analysis for Fault Level Reduction with Inter-Tie Transformer in Designing Power Plant Balikpapan Refinery Project	214
Design of Overcharging Protection and Passive Balancing Circuits Using Dioda for Lithium-Ion Battery Management System	220
The Effect of Ring Radius and Coupling Gap to the Transmission Spectrum of GaN-Based Ring Resonator	224





FACULTY OF
ENGINEERING



The 16th International Conference
on Quality in Research (QiR)

Certificate

This certification is awarded to Mrs./Mr.

Teguh Firmansyah, Gunawan Wibisono and Eko Rahardjo

For acceptance, fully registration, and presentation of the paper with the title of

Compact UWB Bandpass Filter based on Crossed Dumbbell-Stub with Notch Band using Defected Microstrip Structure

In The 16th International Conference on Quality in Research (QiR)
held on 22-24 July 2019 at Padang, West Sumatra.

Universitas Indonesia
Faculty of Engineering Dean,



Dr. Ir. Hendri D.S. Budiono, M.Eng.

QiR 2019 General Chair



Dr. Eng. Muhamad Sahlan

Compact UWB Bandpass Filter based on Crossed Dumbbell-Stub with Notch Band using Defected Microstrip Structure

Teguh Firmansyah
 Department of Electrical Engineering
 Universitas Indonesia
 Depok, Indonesia
 teguh.firmansyah81@ui.ac.id

Gunawan Wibisono*)
 Department of Electrical Engineering
 Universitas Indonesia
 Depok, Indonesia
 gunawan@eng.ui.ac.id

Eko Tjipto Rahardjo
 Department of Electrical Engineering
 Universitas Indonesia
 Depok, Indonesia
 eko@eng.ui.ac.id

Abstract—A compact ultra-wideband (UWB) bandpass filter based on cross dumbbell stub with notch band structures is proposed and implemented. This bandpass filter (BPF) structure consists of directly feed line input/output. As the novelty, the cross dumbbell stub resonator was used and it was placed at the middle of the filter structure. By using this structure, the BPF not only has a compact size but also it has a wide-passband response. To remove unnecessary radio frequency (RF) signal, the rejection (notch) band was also proposed by using a novel technique which uses U-shaped defected microstrip structure (DMS). Moreover, the DMS is constructed at the center between crossed dumbbell resonators. This notch band structure has highly independent and it can be adjusted by modifying the U-shaped structure. Therefore, the specific frequency of the notch band can be selected independently without expanded number of resonator or stub. Furthermore, this BPF is fabricated on 2D - Duroid/RT 5880 substrate with permittivity (ϵ_r) of 2.2, thickness (h) of 1.57 mm, and loss tangent ($\tan \delta$) of 0.0009. Furthermore, the measured results show that the UWB-BPF has 3-dB passband from 3.0 – 12.2 GHz, with notch band at 6.7 GHz and the notch band has attenuation -22 dB. The design structure was verified by a good agreement between simulated and measured result. Overall, the proposed filter design has excellent performance in term of insertion loss, high independent notch-band, compact size, and implementable structures.

Keywords— BPF, defected microstrip structure, crossed-dumbbell, notch, UWB.

I. INTRODUCTION

The ultra-wideband (UWB) wireless technology has great attention after the Federal Communications Commission (FCC) declare that the range of frequency 3.1–10.6 GHz can be used for a commercial purpose [1][2]. The critical subsystem of UWB wireless transceiver is UWB bandpass filter (BPF). High performance of UWB-BPF is needed to reduce noise and interference of radio signals simultaneously. The performance of UWB-BPF can be determined by a good value of insertion loss (S_{21}), compact size, and implementable structures. There are various approaches have been proposed to obtain an excellent performance of UWB-BPF.

The UWB-BPF using modified composite-right/left-handed (CRLH) unit cell is proposed by [3] and to control transmission zeros a cross coupling is used. As the result, this UWB-BPF has good insertion loss (S_{21}) and compact size, but the BPF structure is complex. Furthermore, the cross-coupling with $\lambda/4$ short circuit-stub resonator was used by

[4]. As a result, the proposed UWB-BPF has a compact size and high selectivity.

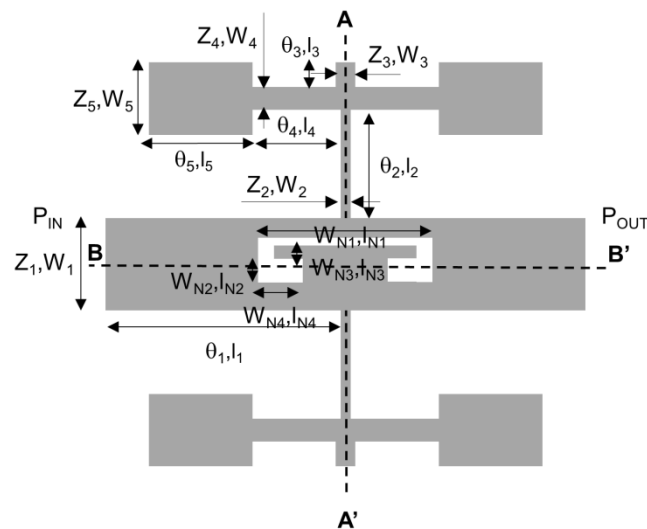


Fig. 1. The proposed UWB-BPF based on Crossed Dumbbell-Stub

The high selectivity response is produced by transmission zeros which are generated by coupling between input and output impedance. Furthermore, a stub-step impedance resonator (SIR) is proposed by [5]. The stub-SIR is connected at its center of filter structure symmetrically. This filter has frequency of 3.1–10.6 GHz. Furthermore, [6] proposed two rectangular stub resonators and single-stage parallel-coupled line and. The rectangular stub resonators create transmission zeros to extend stopband. Moreover, the short-circuited stubs with via-less resonator were investigated by [7]. The resonator structure was investigated by extracting all parasitic elements such as junction and discontinuity to generate UWB BPF. Moreover, Ref [8] presented four resonant modes based on multiple-mode resonator (MMR) with half-mode substrate integrated waveguide (HMSIW) structure. This resonator structure has successfully designed by this resonator structure. However, it has drawback such as complex resonator structure.

Furthermore, the utilizing short-circuited stubs with less-vias resonator structure was proposed by [9]. This paper has advantages such as via less resonator. Another attractive method is proposed by [10]. This paper is investigated UWB-BPF based on one-cell composite right- and left-handed-transmission line (CRLH-TL) resonator with optimized using particle swarm optimization (PSO) process.

However, the UWB-BPF design has drawback such as a complex structure and low selectivity.

In order to remove unnecessary radio frequency (RF) signal, some research proposes the notch band with various resonator structure. Asymmetric open loop resonator with defected ground structures (DGS) was investigated by [11] to produce UWB BPF with notch band. Furthermore, to reduce filter size, the interdigital hairpin resonator unit with three fingers are proposed by [12]. Moreover, the multiple-mode resonators (MMR) and SIR are combined by [13] to increase bandwidth. Another resonator structure to generate UWB BPF with notch band such as complementary split ring resonators (CSRR) [14], embedded SIR [15], radial stub loaded resonator [16], modified non-uniform resonator [17], meander H-shaped slot [18] and multilayer LCP technology [19]. All these methods propose a design UWB-BPF with notch band with good performance of S_{21} . However, the notch band is not independent. Besides that, majority the notch band structure has an impact to extend the filter size.

As novelty, this paper is proposed a compact UWB BPF based on crossed dumbbell-stub with notch band using defected microstrip structure as shown in Fig.1. The contribution of this paper such as: 1) The proposed resonator structure is based on cross dumbbell stub resonator structure, this structure can generate ultrawide pass band, 2) the notch band could be adjusted independently, 3) the notch band resonator is based on U-shaped defected microstrip structure (DMS), so the additional resonator is not required, and 4) the proposed UWB-BPF has excellent performance in term of insertion loss, compact size, and implementable structures.

This paper is organized as follows: Section 2 briefly describes the design of the proposed compact UWB bandpass filter based on crossed dumbbell-stub with notch band using defected microstrip structure, Section 3 presents the simulated and experimental results, and finally, Section 4 concludes this paper.

II. DESIGN OF CROSSED DUMBBELL-STUB RESONATOR WITH NOTCH BAND USING DEFECTED MICROSTRIP STRUCTURE

A. Crossed Dumbbell-Stub Resonator

To generate ultra-wide pass band, the crossed dumbbell stub resonator is proposed, as shown in Fig 1. The crossed dumbbell stub resonator is constructed by dual-dumbbell stub and it is placed at the middle of the filter structure. The W_1 , W_2 , W_3 , W_4 , and W_5 represent the width of the resonator. The l_1 , l_2 , l_3 , l_4 , and l_5 represent the length of the resonator. Furthermore, the resonator structure consists of five transmission lines having different characteristic impedances Z_N ($N = 1,2,3,4,5$) with corresponding electrical lengths θ_N ($N = 5, 1,2,3$), respectively.

Since the resonator is symmetrical to the $A-A'$ plane and $B-B'$ plane, the resonant frequencies for even-mode and odd mode can be determined from impedance condition $Z_{IN} = \infty$ or admittance condition $Y_{IN} = 0$ [20][21][22]. Equivalent circuit model for the even-mode of UWB-BPF is shown in Fig. 2(a) and equivalent circuit model for the odd-mode of UWB-BPF is shown in Fig 2(b).

Analyzing the input impedance of even-mode $Z_{IN-even mode}$ can be derived:

$$Z_{INA} = -jZ_5 \cot \theta_5 \quad (1)$$

$$Z_{INB} = Z_4 \frac{Z_{INA} + jZ_4 \tan \theta_4}{Z_4 + jZ_{INA} \tan \theta_4} \quad (2)$$

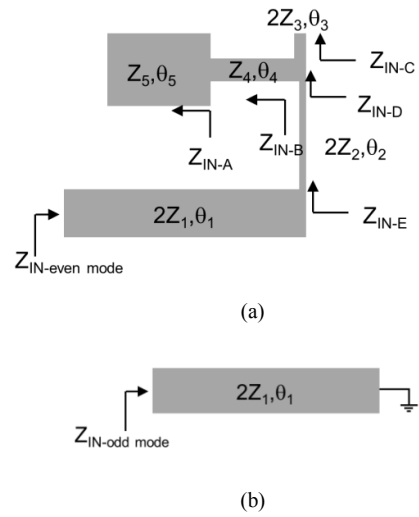


Fig. 2. (a) Equivalent circuit model for the even-mode of UWB-BPF, and (b) Equivalent circuit model for the odd-mode of UWB-BPF.

$$Z_{INC} = -j2Z_3 \cot \theta_3 \quad (3)$$

$$\frac{1}{Z_{IND}} = \frac{1}{Z_{INB}} + \frac{1}{Z_{INC}} \quad (4)$$

$$Z_{INE} = 2Z_2 \frac{Z_{IND} + j2Z_2 \tan \theta_2}{2Z_2 + jZ_{IND} \tan \theta_2} \quad (5)$$

$$Z_{IN-even mode} = 2Z_1 \frac{Z_{INE} + j2Z_1 \tan \theta_1}{2Z_1 + jZ_{INE} \tan \theta_1} \quad (6)$$

Equation (6) can also be expressed as:

$$Z_{IN-even mode} = \frac{2Z_1 A + j4Z_1^2 B \tan \theta_1}{2Z_1 B + jA \tan \theta_1} \quad (7)$$

with:

$$A = 2Z_2 Z_{IND} + j4Z_2^2 \tan \theta_2 \quad (8)$$

$$B = 2Z_2 + jZ_{IND} \tan \theta_2 \quad (9)$$

and:

$$Z_{IND} = \frac{P - Q}{R + S + T - U} \quad (10)$$

where :

$$P = 2Z_3 Z_4 Z_5 \cot \theta_3 \cot \theta_5 \quad (11)$$

$$Q = 2Z_3 Z_4^2 \cot \theta_3 \tan \theta_4 \quad (12)$$

$$R = j2Z_3 Z_4 \cot \theta_3 \quad (13)$$

$$S = j2Z_3 Z_5 \cot \theta_3 \cot \theta_5 \tan \theta_4 \quad (14)$$

$$T = jZ_4 Z_5 \cot \theta_5 \quad (15)$$

$$U = jZ_4^2 \tan \theta_4 \quad (16)$$

The resonant frequencies can be obtained when:

$$2Z_1 B + jA \tan \theta_1 = 0 \quad (17)$$

Analyzing the input impedance of odd-mode $Z_{IN-odd mode}$ can be derived:

$$Z_{IN-odd mode} = j2Z_1 \tan \theta_1$$

The resonant frequencies odd mode can be determined from impedance condition $Z_{IN} = \infty$. The condition of the structure is found as follows

$$\tan \theta_1 = \infty \quad (18)$$

$$\theta_1 = \frac{(2n-1)}{2}\pi; \text{ for } n = 1, 2, 3 \dots \quad (19)$$

Furthermore, the next step is to add the effect of the notch resonator.

B. Notch Band using Defected Microstrip Structure (DMS)

In order to remove unnecessary radio frequency (RF) signal, the rejection (notch) band was also proposed by using U-shaped defected microstrip structure (DMS). Moreover, the DMS is constructed at the center of crossed dumbbell resonator, as shown in Fig 3.

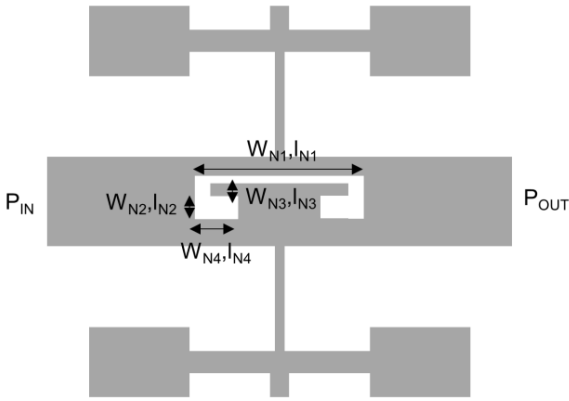


Fig. 3. The proposed defected microstrip structure (DMS) for notch band application

The W_{N1} , W_{N2} , W_{N3} , and W_{N4} , represent the width of the DMS resonator. The l_{N1} , l_{N2} , l_{N3} , and l_{N4} represent the length of the DMS resonator. The simulation and optimization is done by using The Momentum Advanced Design System (ADS). As a result, Fig 4 shows the insertion loss (S_{21}) response with varied W_{N3} (mm). Furthermore, Fig 5 shows the return loss (S_{11}) response with varied W_{N4} (mm). Fig 4. indicates that by increasing W_N , the frequency notch band is unchanged. However the value of S_{21} will increase slightly, but the attenuation is still lower than -15 dB.

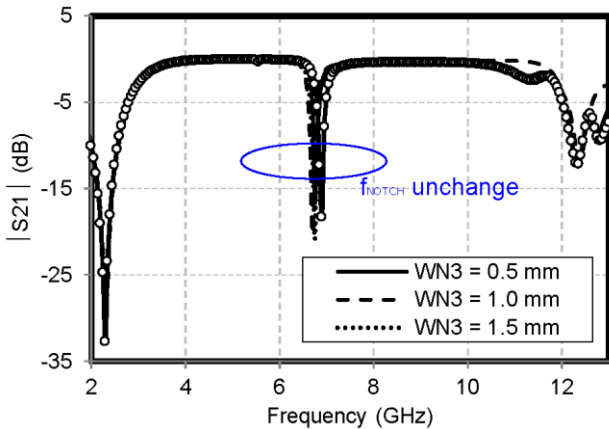


Fig 4. S_{21} (dB) response with varied W_{N3}

Fig 5 shows that by increasing W_{N3} the frequency notch band is still stable. However the frequency value at the lowest S_{11} will shift slightly, but the value of S_{11} has still lower than -30 dB. The figure also shows that the cutoff frequency at upper and lower band unchanged.

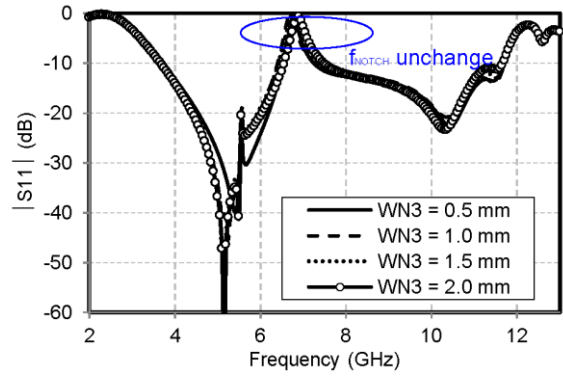


Fig 5. S_{11} (dB) response with varied W_{N3}

Furthermore, Fig 6 and Fig 7 show the S_{21} and S_{11} response with varied W_{N4} , respectively. The illustration from Fig 6, we can see that the frequency notch band is shifted independently. Although, there is a change in the notch band frequency, the upper and lower cut off frequency value remain stable. Therefore, the notch band frequency can be adjusted by modifying the U-shaped structure in term of W_{N4} . Moreover, the DMS method could produce the specific notch band without an expanded number of resonator or stub.

Moreover, Fig 7 shows the S_{11} (dB) response with varied W_{N4} . The data indicates that by increase a value of W_{N4} , the frequency of the notch band will be shifted to higher frequency. It is interesting to note that, the change in the value of frequency notch band by varied W_{N4} , was not accompanied by changes in the value of upper and lower frequency cutoff.

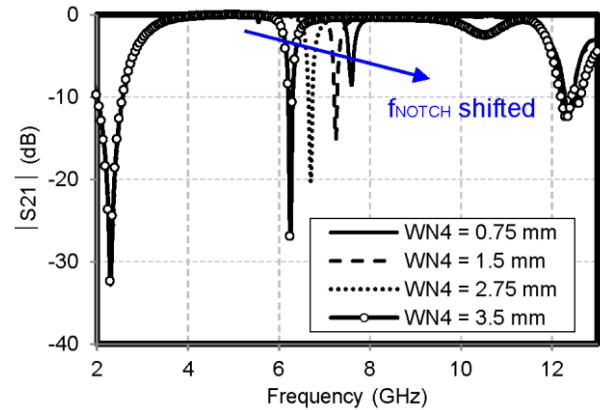


Fig 6. S_{21} (dB) response with varied W_{N4}

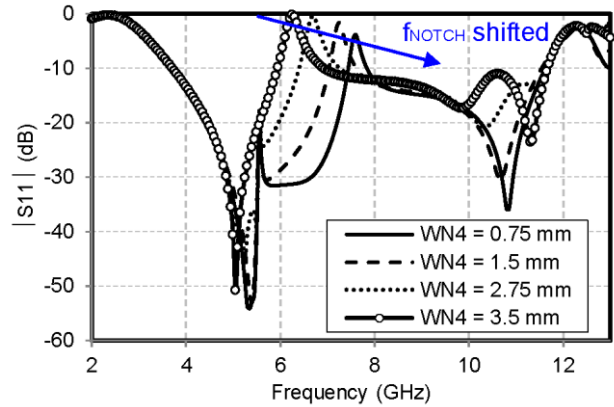


Fig 7. S_{11} (dB) response with varied W_{N4}

III. IMPLEMENTATION OF CROSSED DUMBBELL-STUB RESONATOR WITH NOTCH BAND USING DEFECTED MICROSTRIP STRUCTURE

To validate the propose method, the prototype of BPF has been designed, built, and tested as shown in Fig 8a and 8b. Fig 8a and 8b show the photograph of UWB-BPF and UWB-Notch BPF, respectively. This BPF is fabricated on 2D - Duroid/RT 5880 substrate with permittivity ϵ_r of 2.2, thickness h of 1.57 mm, and loss tangen tand of 0.0009.

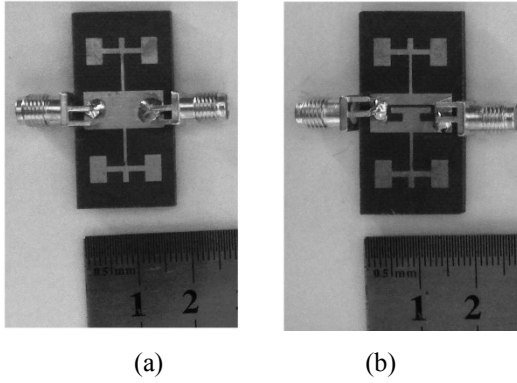
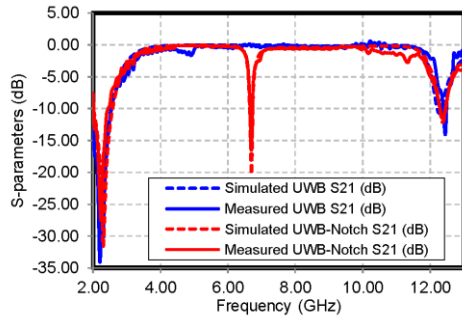
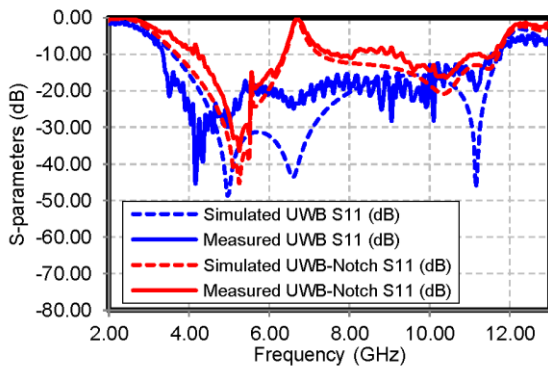


Fig 8. The photograph of (a) UWB-BPF and (b) UWB-Notch BPF.

Furthermore, after optimization, the following dimension of filter structure was fabricated: $W_1 = 7$ mm, $W_2 = 0.5$ mm, $W_3 = 1$ mm, $W_4 = 1$ mm, and $W_5 = 5$ mm. The $l_1 = 7.25$ mm, $l_2 = 7$ mm, $l_3 = 2$ mm, $l_4 = 3.5$ mm, and $l_5 = 3$ mm. Moreover, the size of $W_{N1} = 0.5$ mm, $W_{N2} = 0.75$ mm, $W_{N3} = 1$ mm, and $W_{N4} = 1.5$ mm, represent the width of the DMS resonator. The $l_{N1} = 8.5$ mm, $l_{N2} = 1.5$ mm, $l_{N3} = 2$ mm, and $l_{N4} = 2.75$.



(a)



Figs. 9. Comparison of imulation and measurement results of (a) S_{21} , and (b) S_{11}

Fig 9 (a) shows the comparison between simulation and measurement S_{21} results achieved by the UWB-Notch BPF.

A VNA Rohde Schwarz ZVA67 was used to test the fabricated prototype. Both simulated and measured results of the UWB-BPF have accomplished UWB requirements with a frequency range of 3.0 – 12.2 GHz. The S-parameters is slightly shifted due to the imperfection of soldering and pabrication process. Moreover, the measured result of UWB-Notch BPF has addition the notch band at 6.7 GHz with attenuation more than -20 dB. This notchband can be adjusted independently.

Fig 10(a) and 10(b) show the surface current distribution of lower band UWB-NotchBPF and upper band UWB-Notch BPF, respectively. The important information for the RF signal flows can be determined by plotting the surface current distribution. The surface current of UWB-BPF has been investigated by Momentum-ADS. The surface current distribution at the lower frequency band has flowed at the lower resonator, as shown in Fig 10(a). Furthermore, the surface current distribution at the upper frequency band has flowed at the upper resonator as shown in Fig 10(b). Moreover, Table 1 summarizes the comparison of the proposed UWB-BPF.

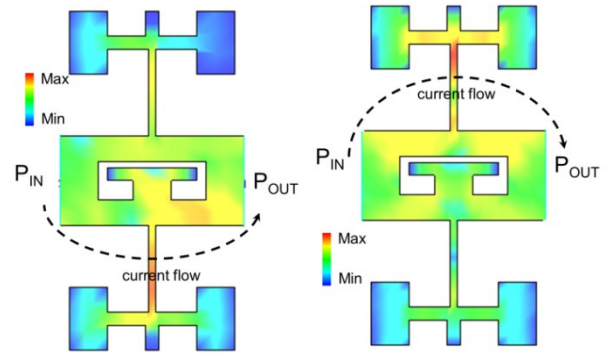


Fig. 10. Surface current distribution on of (a) lower band UWB-NotchBPF and (b) upper band UWB-Notch BPF.

Table 1. Summarizes the comparison of the proposed UWB-BPF

Ref	3 dB Pass-band (GHz)	ϵ_r / h	Notch freq (GHZ)/attenuation (dB)	Structure / Independent notch	Size $\lambda_G \times \lambda_G$ (λ_G : at 6.85 GHz)
[15]	3.1 – 10.6	2.2 / 0.78	5.22 / 20	2-D / no	0.61 x 0.50
[16]	3.0 – 10.8	2.2 / 0.50	8.1 / 20	2-D / no	0.55 x 0.35
[17]	3.6 – 10.2	10.8 / 0.63	5.6 / 15	2-D / no	0.82 x 0.17
[18]	2.8 - 10.8	2.65 / 1.0	5.47 / 20	2-D / no	0.82 x 0.36
[19]	2.6 - 10	3.15 / NA	6.4 / 8.0	3-D / no	1.36 x 0.32
Proposed 1	3.0 – 12.2	2.2 / 1.57	-	2-D / NA	0.42 x 0.84
Proposed 2	3.0 – 12.2	2.2 / 1.57	6.7 / 22	2-D / yes	0.42 x 0.84

NA = Not available

IV. CONCLUSION

A compact ultra wideband (UWB) bandpass filter based on cross dumbbell stub with notch band structures is successfully implemented, and measured. In order to remove unnecessary radio frequency (RF) signal, the rejection

(notch) band was also proposed by using DMS. This BPF is fabricated on 2D - Duroid/RT 5880. The measured results show that the UWB-Notch has 3-dB passband from 3.0 – 12.2 GHz, with notchband at 6.7 GHz and the notch band has attenuation -22 dB. The design structure was verified by good agreement between simulated and measured result. In conclusion, the proposed filter design has excellent performance in term of insertion loss, high independent notch-band, compact size, and implementable structures.

ACKNOWLEDGMENT

The authors would like to thank Universitas Indonesia for funding through Hibah PIT9 Universitas Indonesia (UI), under contract No. NKB-0299/UN.R3.1/HKP.05.00/2019

REFERENCES

- [1] J. Liu, J. Lu, Z. He, T. Luo, X. Ying, and J. Zhao, "Super Compact Microstrip Uwb Bpf With Triple-Notched Bands," *Prog. Electromagn. Res. Lett.*, vol. 73, no. November 2017, pp. 61–67, 2018.
- [2] H. Peng, J. Zhao, and B. Wang, "Compact Microstrip Uwb Bandpass Filter With Triple-Notched Bands and Wide Upper Stopband," *Prog. Electromagn. Res.*, vol. 144, no. January, pp. 185–191, 2014.
- [3] J.-Q. H. and Q.-X. Chu, "Compact UWB Band-Pass Filter Utilizing Modified Composite Right/Left-Handed Structure With Cross Coupling," *Prog. Electromagn. Res. B*, vol. 29, pp. 269–288, 2011.
- [4] X. Li and X. Ji, "Novel compact UWB bandpass filters design with cross-coupling between $\lambda/4$ short-circuited stubs," *IEEE Microw. Wirel. Components Lett.*, vol. 24, no. 1, pp. 23–25, 2013.
- [5] A. Taibi, M. Trabelsi, A. Slimane, M. T. Belaroussi, and J. P. Raskin, "A novel design method for compact UWB bandpass filters," *IEEE Microw. Wirel. Components Lett.*, vol. 25, no. 1, pp. 4–6, 2015.
- [6] S. W. Lan, M. H. Weng, C. Y. Hung, and S. J. Chang, "Design of a Compact Ultra-Wideband Bandpass Filter with an Extremely Broad Stopband Region," *IEEE Microw. Wirel. Components Lett.*, vol. 26, no. 6, pp. 392–394, 2016.
- [7] M. S. Razalli, A. Ismail, M. A. Mahdi, and M. N. bin Hamidon, "Novel Compact Microstrip Ultra-Wideband Filter Utilizing Short-Circuited Stubs With Less Vias," *Prog. Electromagn. Res.*, vol. 88, pp. 91–104, 2008.
- [8] C. X. Zhou, P. P. Guo, K. Zhou, and W. Wu, "Design of a Compact UWB Filter with High Selectivity and Superwide Stopband," *IEEE Microw. Wirel. Components Lett.*, vol. 27, no. 7, pp. 636–638, 2017.
- [9] M. S. Razalli, A. Ismail, M. A. Mahdi, and M. N. bin Hamidon, "Novel Compact 'Via-Less' Ultra-Wide Band Filter Utilizing Capacitive Microstrip Patch," *Prog. Electromagn. Res.*, vol. 91, pp. 213–227, 2009.
- [10] Y. C. Yun, S. H. Oh, J. H. Lee, K. Choi, T. K. Chung, and H. S. Kim, "Optimal Design of a Compact Filter for UWB Applications Using an Improved Particle Swarm Optimization," *IEEE Trans. Magn.*, vol. 52, no. 3, pp. 1–4, 2016.
- [11] P.-Y. Hsiao and R.-M. Weng, "Compact Open-Loop UWB Filter With Notched Band," *Prog. Electromagn. Res. Lett.*, vol. 7, pp. 149–159, 2009.
- [12] F. Wei and L. Chen, "Compact UWB Bandpass Filter With Notched Band," *Prog. Electromagn. Res. C*, vol. 4, pp. 121–128, 2008.
- [13] N. Daryasafar, S. Hamidi, and G. R. Shahryari, "Design and analysis of an ultra-wideband band-notched band-pass filter," *J. Electr. Eng.*, vol. 66, no. 2, pp. 113–116, 2015.
- [14] H. Lin, X. Xia, Z. Guo, and T. Yang, "Compact Uwb Filter With High Selectivity and a Deep Notched Band," *Prog. Electromagn. Res. Lett.*, vol. 63, no. October, pp. 123–128, 2016.
- [15] R. Ghatak, P. Sarkar, R. K. Mishra, and D. R. Poddar, "A compact UWB bandpass filter with embedded SIR as band notch structure," *IEEE Microw. Wirel. Components Lett.*, vol. 21, no. 5, pp. 261–263, 2011.
- [16] J. Xu, W. Wu, W. Kang, and C. Miao, "Compact UWB bandpass filter with a notched band using radial stub loaded resonator," *IEEE Microw. Wirel. Components Lett.*, vol. 22, no. 7, pp. 351–353, 2012.
- [17] S. W. Wong and L. Zhu, "Implementation of compact UWB bandpass filter with a notch-band," *IEEE Microw. Wirel. Components Lett.*, vol. 18, no. 1, pp. 10–12, 2008.
- [18] G. M. Yang, R. Jin, C. Vittoria, V. G. Harris, and N. X. Sun, "Small Ultra-wideband (UWB) bandpass filter with notched band," *IEEE Microw. Wirel. Components Lett.*, vol. 18, no. 3, pp. 176–178, 2008.
- [19] Zhang-Cheng Hao and Jia-Sheng Hong, "Compact UWB Filter With Double Notch-Bands Using Multilayer LCP Technology," *IEEE Microw. Wirel. Components Lett.*, vol. 19, no. 8, pp. 500–502, 2009.
- [20] T. Firmansyah, S. Praptodinyo, R. Wiryadinata, S. Suhendar, S. Wardoyo, A. Alimuddin, C. Chairunissa, M. Alaydrus, and G. Wibisono, "Dual-wideband band pass filter using folded cross-stub stepped impedance resonator," *Microw. Opt. Technol. Lett.*, vol. 59, no. 11, 2017.
- [21] T. Firmansyah, S. Praptodiyono, A. S. Pramudyo, C. Chairunissa, and M. Alaydrus, "Hepta-band bandpass filter based on folded cross-loaded stepped impedance resonator," *Electron. Lett.*, vol. 53, no. 16, 2017.
- [22] H. Wu and R. Yang, "A New Quad-Band Bandpass Filter Using Asymmetric Stepped Impedance Resonators," vol. 21, no. 4, pp. 203–205, 2011.